Structural analysis of bellcrank in a pullrod suspension system in an FSAE prototype

Abhishek Mahesh Sharma[1], Sidhant Konwar Roy[2], AnanthaKrishnan R[3], Nivedh Das Thaikoothattil[4]

[1-4] Department of Mechanical Engineering, R V College of Engineering

[1] abhishekms.me17@rvce.edu.in, [2]sidhantkr09@gmail.com, [3]krishnan071999@gmail.com, [4]nivedhdast.me17@rvce.edu.in

Abstract: The cause of accidents due to suspension failure is fatigue. The goal of this project was to design a bell crank for an FSAE prototype to withstand fatigue loads and reduce the chances of failure during its use. After finding the bellcrank forces, the dimensions of the bellcrank and the associated OEMs (bearings) are calculated and found. This was followed by CAD modelling and structural optimization using Autodesk Fusion 360 software. Finally, finite element analysis was performed and a comparative study was done between the new and old model of bellcrank assembly based on mass, fatigue life and factor of safety and the results were acknowledged.

Keywords: **Bellcrank, FSAE, Fatigue, Pull-rod suspension system, Structural Optimization**

Introduction

Typically, a vehicle has two types of mass: sprung mass and an unsprung mass. The ratio of sprung to unsprung is essential in understanding the vertical dynamics of the vehicle. Generally, it is recommended to have a high sprung to unsprung mass ratio (about 4 to 6). To achieve this, the ratio of the two is tweaked by altering the sprung mass or unsprung mass. It is recommended to decrease the unsprung mass as compared to increase in sprung mass as the latter increases the overall weight of the vehicle. In automotive engineering, mass plays a crucial role in the overall performance of the vehicle. The Bellcrank is a mechanical lever which is used to change the direction of motion and magnitude of force which acts on the effort end of the lever. The effort end of the lever is connected to a push/pull rod of the suspension linkage assembly. The load ends of the lever are connected to the shock absorber and the anti-roll bar which in turn is connected to the chassis of the vehicle. In the FSAE community, various attempts have been made in reducing unsprung mass by using various techniques to improve vehicle performance including ride and handling. In this paper, a bellcrank of a pull rod suspension system with a given mechanical advantage and motion ratio will be designed which will be lighter and stronger than the currently used bellcrank in the FSAE community shown in figure 1.

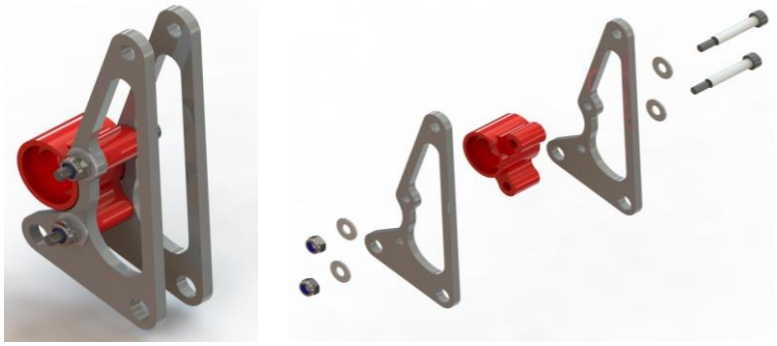

Fig 1. Existing Bellcrank Design in FSAE

Calculation of Forces acting on the bellcrank

Suspension Linkage Force Calculation is based on Newton's First Law of motion. The various suspension points on which the forces act was obtained from an FSAE team. The bellcrank force calculation is based on the Principle of Moments where forces acting at effort and load end are equated about the fulcrum. Since the end points of the suspension linkages are pin joints, they restrict motion only about the axial direction. Hence the force direction is about the axial direction of the linkage. The direction of the linkage is known from the end point coordinates of the linkage; hence the direction of the force vector can be known. The unknown quantities are the magnitude of forces. There are 6 unknowns (2 for lower a-arm, 2 for upper a-arm, 1 for pull rod and 1 for tie rod), for which 6 equations will be needed to solve for the unknowns. The direction vectors of the links and the moment due to the linkage force about the origin of the coordinate system by taking the cross product of the radius vector and direction force vector need to be found. The tire forces and moments that act on the origin of the coordinate system are equated. From that, 6 equations are obtained and using the matrix method, the unknowns are solved. Once the pull rod force is known, using the principle of moments, the damper force and arb (anti roll bar) droplink force can be calculated. The fulcrum force is the vector sum of pullrod force, damper force and arb force.
The table 1 shown below are the forces acting on the bellcrank

Table 1. Forces acting on the bellcrank

	X direction	Y direction	Z direction	Units
Pullrod force	0	1988	1650	N
Damper force	0	1920	24	N
ARB force	0	-4595	0	N
Fulcrum force	0	-687	1674	N

Selection of suitable material for the bellcrank

Materials used in suspension components must be durable, strong, stiff and cheap. As suspension components are subjected to dynamic loads, the material must have a high fatigue strength as well. Keeping all these conditions in mind, bellcrank material must have high young's modulus, high yield strength, high fatigue strength, low density and low cost. Comparative study was done to choose the most suitable material from a given set of materials by the method of weights. In this method, equal weights of 100 points were assigned to every parameter (strength, density and cost). The most desired value among the set of materials for a given parameter is compared with the value of the given material and weights are assigned accordingly.
Table 2 shows the material and its corresponding parameter values for the comparative study and Table 3 shows the result of the comparative study.

Table 2. Material properties and its cost

	Yield Strength GPa	Young's Modulus GPa	Fatigue Strength MPa	Density g/cm3	Cost (Rupees/kg)
Titanium 6Al-4V Grade 5	880	113.5	240	4.43	1200
Aluminium 2014 T6	414	72.4	124	2.8	600
Aluminium 7075 T6	503	71.7	159	2.81	800
Aluminium 6061 T6	450	68.9	140	2.71	350
Mild Steel AISI 1018	370	200	200	7.87	75
Best	880	200	240	2.71	75
Worst	370	68.9	124	7.87	1200

Table 3. Results of Comparative study

Weights	Yield Strength	Young's Modulus	Fatigue Strength	Density	Cost	Total
Titanium 6Al-4V Grade 5	100	57	100	61	0	318
Aluminium 2014 T6	47	36	0	97	13	193
Aluminium 7075 T6	57	36	66	96	9	264
Aluminium 6061 T6	51	0	58	100	21	230
Mild Steel AISI 1018	0	100	83	0	100	283

Sample calculation is shown below for points assigned to Titanium 6Al-4V Grade 5 alloy:

1. For Yield Strength, points=100 as that alloy has the highest yield strength.
2. For Young's Modulus, points= (113.5/200) *100=57
3. For Fatigue Strength, points=100 as that alloy has the highest fatigue strength.
4. For density, points= (2.71/4.43) *100=61
5. For cost, points=0 as that alloy is the costliest among the set of materials.
6. Total points=100+57+100+61+0=318.

From table 3, it is observed that Titanium 6Al-4V Grade 5 alloy has the highest total points when compared to other materials in the set. Hence Titanium 6Al-4V Grade 5 alloy was chosen for this project.

Determination of the bellcrank dimensions

The bellcrank requires a needle roller bearing at the fulcrum to restrict its motion (to only have a rotational degree of freedom about the local Y axis). The pull rod and the arb droplink are connected to the effort and load ends of the bellcrank respectively using rod end bearings.

The rod end bearings are chosen based on the static load capacity of the bearing. Let's find the bearing that goes into the arb droplink as the force acting on that link is the highest. The force acting on the arb droplink is F=(4600j) N. In order to calculate the static load capacity, the following formula was used:

Static Load Capacity=Force*Factor of Safety. Static Load Capacity=4600*1.5=6900 N.

Since rod ends don't rotate, required dynamic load capacity is zero. GAKR6-PW bearing was chosen at the arb droplink end and pull rod end.

The needle roller bearing is chosen based on static and dynamic load capacity. The force acting on the fulcrum is (-687j+1474k) N which has a magnitude of 1810 N. 1810 N is the radial force that is acting on the bearing with no axial force. Since only radial force is acting on the bellcrank, needle roller bearing was used. Taking the radial factor, thrust factor and rotation factor to be 1.0, 0.0 and 1.2 respectively for calculations. The calculations are shown below:

Static Load Capacity=1.5*Radial Factor*Rotation Factor*Radial Force

Static Load Capacity=1.5*1.0*1.2*1810=3258 N

Expected Life=2.7 million cycles.

Dynamic Load Capacity= (Expected Life$^{0.3}$)*Static Load Capacity

Dynamic Load Capacity= (2.70.3) *3258=4389N

Based on the above calculations, NK8/16-TV-XL bearing was considered.

From the product datasheets of the NK8/16-TV-XL bearing and GAKR6-PW bearing, critical dimensions were noted which were used to alter the dimensions of the bellcrank model.

After selecting the material and desired OEM, the dimensions of the component were to be found. This is done based on the design stress value. The loads that were calculated previously and titanium 6Al-4V alloy were taken into consideration for the design calculations of the bellcrank model. As per FSAE rules, bolts must have a grade of 8.8 and above. Hence a 12.9 grade bolt was chosen. A factor of safety of 5 was chosen for bolts as these are critical components which are subjected to dynamic loading. A factor of safety of 4 was chosen for the lever as this component is subjected to dynamic loading.

Table 4 shows the results of the calculations performed to find bellcrank pin dimensions.

Design of Fulcrum pin (Based on Bearing Stress)			
Fulcrum pin diameter or shank diameter of bolt	d	3	mm
Calculated Length of Fulcrum Pin	L	3.75	mm

Design of Effort pin (Based on Bearing Stress)			
Effort pin diameter or shank diameter of bolt	d	4	mm
Length of the bolt	L	5	mm

Design of Load pin (damper) based on bearing stress			
Load pin diameter or shank diameter of bolt	d	3	mm
Length of the bolt	L	3.75	mm

Design of Load pin (arb) based on bearing stress			
Load pin diameter or shank diameter of bolt	d	5	mm
Length of bolt	L	6.25	mm

Table 4. Bellcrank Pin Dimension Calculation

All the bearings used in the bellcrank are known. The dimensions of the pins (bolts) which were determined previously are altered based on the dimensions of the OEMs (Rod end bearing and Needle Roller bearing). After making changes to the dimensions, a safety check is done. The safety check is done based on the shear stress acting on the bolts or pins at the fulcrum end, effort end and load ends of the bellcrank. The pin is safe when the shear stress acting on the pin is less than the shear strength of the pin material. The table 5 shows whether the bellcrank pins are safe.

Table 6 shows the bellcrank bolts used.

Fulcrum Pin							
Fulcrum pin diameter or shank diameter of bolt	d	8	mm	Shear stress at pin	17.99	MPa	Safe
Effort Pin							
Pin diameter or shank diameter of bolt	d	6	mm	Shear stress at pin	45.69	MPa	Safe
Load Pin (damper)							
Pin diameter or shank diameter of bolt	d	6	mm	Shear stress at pin	33.97	MPa	Safe
Load Pin (arb)							
Pin diameter or shank diameter of bolt	d	6	mm	Shear stress at pin	81.24	MPa	Safe

Table 5. Check for Safety of bellcrank pins

DIMENSION OF PINS/BOLTS			
Fulcrum pin			
Diameter	d	8	mm
Effort pin			
Diameter	d	6	mm
Load (damper) pin			
Diameter	d	6	mm
Load (arb) pin			
Diameter	d	6	mm

Table 6. Dimensions of Pins/Bolts

After the pin dimensions are finalized, the bellcrank dimensions are found based on OEM dimensions, pin dimensions, bearing and shear stress. The outer diameter of the fulcrum is based on the bending stress that acts on the fulcrum due to the loads. The table 7 shows the dimensions of the bellcrank fulcrum Given information:

- Inner diameter of NK8/16-TV-XL bearing is 8mm (From product datasheet).
- Outer diameter of NK8/16-TV-XL bearing is 15mm (From product datasheet).
- Length of NK8/16-TV-XL bearing is 16mm (From product datasheet).
- Inner diameter of fulcrum=outer diameter of NK8/16-TV-XL bearing=15mm.

Design of Fulcrum			
Fulcrum pin diameter or shank diameter of bolt	d	8	mm
Calculated Length of fulcrum pin or length of shank in bolt	L	10	mm
Actual Length of fulcrum pin or length of shank in bolt	l	16	mm
Calculated inner diameter of fulcrum	Dri	16	mm
Actual inner diameter of fulcrum	Di	15	mm
Bending moment	M	124038.54	N-mm
Section modulus of fulcrum	Z	563.81	mm
Outer diameter of fulcrum	Do	22	mm

Table 7. Fulcrum Dimensions calculation

After finding the fulcrum dimensions, the rocker plate dimensions (diameter and thickness) are calculated based on OEM dimensions, pin dimensions and normal stress acting at the effort and load ends of the bellcrank.

Table 8 shows the dimensions of the rocker plate.

Design of plate (rocker plate)			
Effort hole diameter	de	8	mm
Outer diameter at effort end	De	16	mm
Stress Concentration Factor	K	2.2	
Thickness at effort end	te	4	mm
Load(damper) hole diameter	dld	6	mm
Outer diameter at load(damper) end	Dld	12	mm
Stress Concentration Factor	K	2.2	
Thickness at load(damper) end	tld	4	mm
Load(arb) hole diameter	dla	8	mm
Outer diameter at load(arb) end	Dla	16	mm
Stress Concentration Factor	K	2.2	
Thickness at load(arb) end	tla	6	mm
Thickness of plate	t	6	mm
Thickness of rocker plate	te	3	mm
Gap between plates (in case of double shear)	g	14	mm

Table 8. Dimensions of the rocker plate region of bellcrank

After the dimensions are calculated, modelling is carried out.

Modelling and Structural Optimization of the Bellcrank

Using the dimensions of bellcrank calculated, modelling was done on Autodesk Fusion 360.
The figures 2a, 2b and 2c shown below are the different views of the CAD model of the bellcrank

Fig 2a. Isometric View

Fig 2b. Front View

Fig 2c. Side View

Structural Optimization is a process of enhancing the performance of a structure by reducing material, mass and overall cost of the structure without compromising on its functionality. This process works in the principle of Finite Element Methods. Autodesk Fusion 360 software was used for the structural optimization of the bellcrank. On importing the geometry, the CAD model was discretized (meshed). Tetrahedron elements of size 1 mm were used in the study. After meshing, boundary conditions were applied. Boundary conditions include:

1. Fixed support (Ux=Uy=Uz=Mx=My=Mz=0) at the cylindrical surface of the load end holes having a diameter of 6mm and 8mm respectively where the damper and the ARB (Anti Roll Bar) droplink is attached on the bellcrank.
2. Cylindrical Support or Revolute Joint (Ux=Uy=Uz=Mx=Mz=0) at the cylindrical surface of the fulcrum hole having a diameter of 15mm.
3. Force on the cylindrical surface of the effort hole having a diameter of 8mm. The force is represented in vector form: (0i + 1988j + 1650k) N. Now certain design criteria were kept during the optimization study. They include mass reduction of 60%, maximum stiffness and minimum member size of 3mm. Figure 3 shows the boundary condition for the optimization study and figure 4 shows the load path.

Fig 3. Boundary Conditions

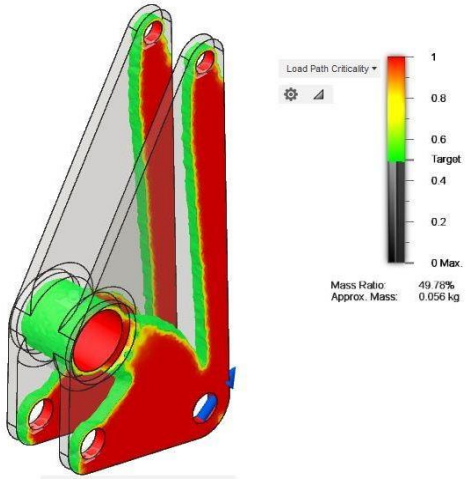

Fig 4. Load path

The final optimized CAD model obtained after the optimization process is shown in figure 5a, 5b and 5c.

Fig 5a. Isometric View

Fig 5b. Front View

Fig 5c. Side View

Simulation of the bellcrank model

Once the CAD model is optimized, simulation must be performed to ensure that the component won't fail under loading. The software used for simulation is ANSYS. The model is discretized into multiple tetrahedron elements (3D elements). Since all 3 dimensions of the geometry were comparable to each other, 3D elements were considered for this simulation study. The reason why tetrahedron elements were chosen over other choices is because they have better numerical properties, where what constitutes a "better" element. This depends on the general governing equations and the particular solution to the model instance in comparison to a pyramid. Choosing such an element also aids in bringing the aspect ratio closer to one. Once the mesh is generated, the mesh quality is a critical information that tells us the quality of the mesh and whether the mesh will generate accurate results. The tabular column 9 below is the mesh quality of the generated mesh on the geometry.

Table 9. Mesh Quality

Mesh Quality	Element Quality	Aspect Ratio	Jacobian Ratio	Max corner angle	Skewness	Orthogonal Quality	Characteristic length
MIN	0.25	1.16	1	70.845	0.000062	0.039	0.21mm
MAX	0.99	7	6.3	152.23	0.96	0.989	2.28mm
AVG	0.76	2.08	1.02	100.53	0.336	0.66	1.0667mm
STD	0.12	0.6061	0.07	13.518	0.178	0.17	0.325mm

The maximum number of elements in the meshed geometry is 75661. The maximum number of nodes in the meshed geometry is 124781. Figure 6 shows the discretization of the CAD model.

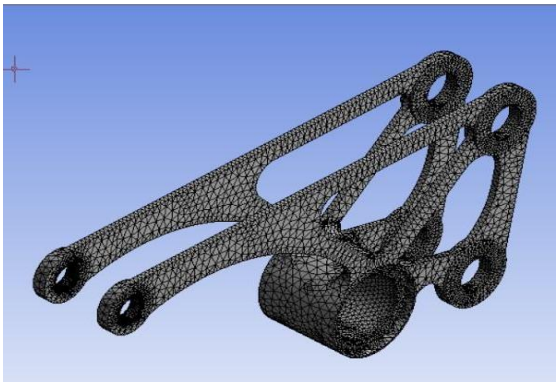

Fig 6. Meshing

After the mesh is generated, boundary conditions must be applied on different regions of the geometry. Boundary conditions similar to that used in structural optimization were used. Once the boundary conditions are provided on the nodes of the meshed geometry, the simulation study is solved. Figure 7 and Figure 8 show the boundary condition of the simulation.

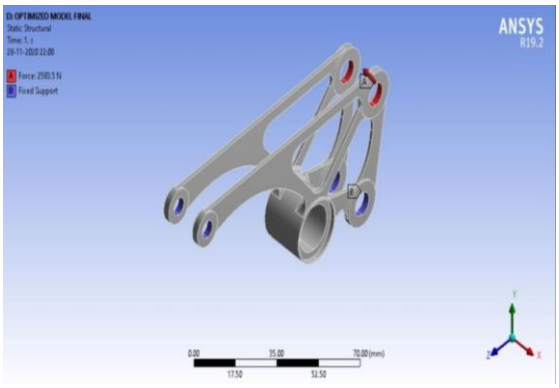

Fig 7. Boundary Conditions

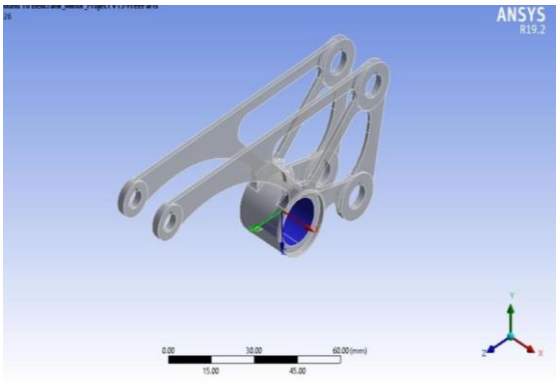

Fig 7. Boundary Conditions (Revolute Joint at Fulcrum)

Different results were graphically shown such as Von Mises Stress (Figure 8), Total Deformation (Figure 9), Convergence (Fig.10) Static Factor of Safety (Figure 11) and Fatigue life (Figure 12).

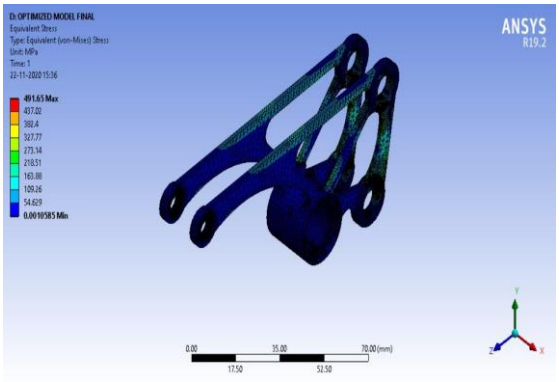

Fig 8. Von Mises Stress

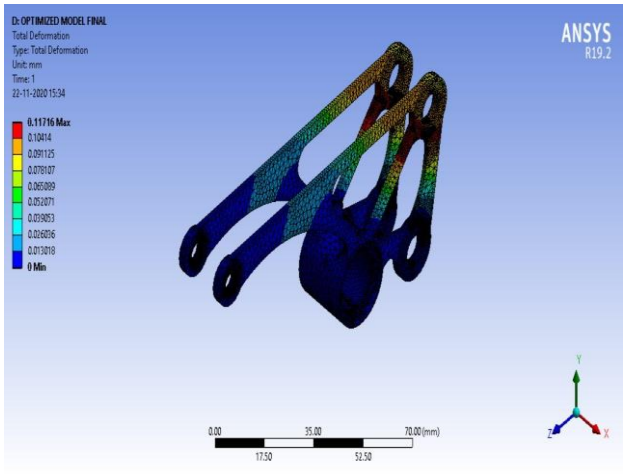

Fig 9. Total Deformation

To check the accuracy of the result, a convergence study (Figure 7.6) was done on Von Mises Stress acting on the component. The results of the study conclude that the solution is converged and a variation of -0.22% in stress is observed for different values of elements.

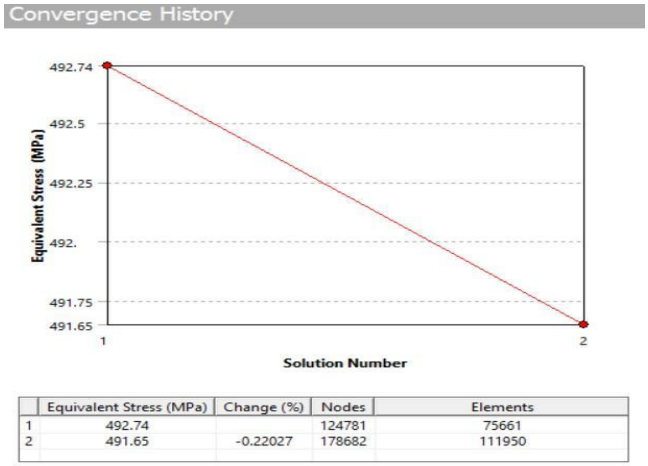

	Equivalent Stress (MPa)	Change (%)	Nodes	Elements
1	492.74		124781	75661
2	491.65	-0.22027	178682	111950

Fig 10. Convergence

Table 10 shows the Total Deformation and Von Mises Stress in tabular form.

Table 10. Total Deformation and Von Mises Stress

Results	Max	Min	Unit
Total Deformation	0.11	0	mm
Von Mises Stress	491.65	0.001	MPa

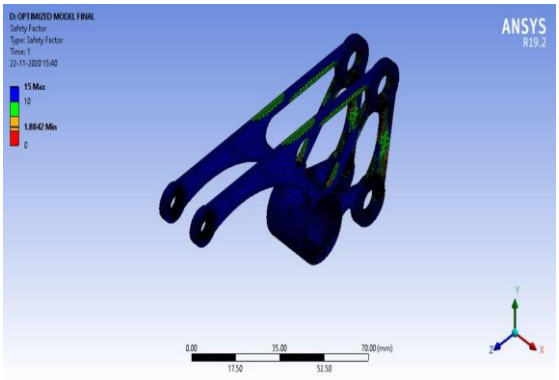

Fig 11. Static Factor of Safety

The static failure theory used was Coulomb-Mohr Failure Theory and the reason for selecting this failure theory is because Titanium 6Al-4V Grade 5 alloy is brittle material.

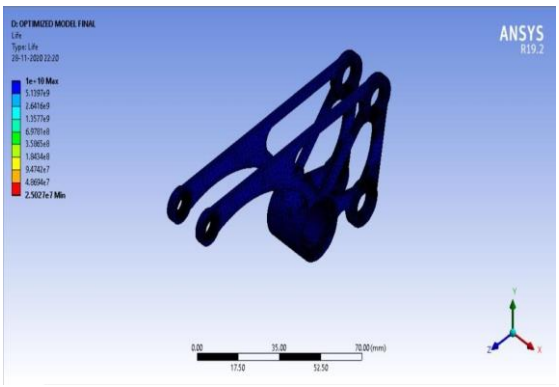

Fig 12. Fatigue Life

The fatigue failure theory used was Goodman Failure Theory and the reason for selecting this failure theory is because the material chosen is brittle. As the static and fatigue factor of safety is greater than unity, this means that the component will not fail under loading.

Table 11 shows the Total Deformation and Von Mises Stress in tabular form.

Table 11. Static Factor of Safety and Fatigue Life

Result	Min	Max	Unit
Static Factor of Safety	1.88	15.0	-
Fatigue Life	2.503×10^{7}	1×10^{10}	cycles

Results: Performance Comparison between old and new bellcrank design

After completing the simulation of the new design, a performance comparison is done with the old design to see the benefits of the new design. Despite having higher compliance in the new bellcrank, the motion ratio achieved due to compliance is progressive which is useful in automotive suspension systems. Table 12 shows the performance comparison.

Table 12. Performance Comparison between old and new bellcrank

Parameter	Old Bellcrank	New Bellcrank
Material	Al 7075	Ti-6Al-4V
Mass	86.56 g	39.9 g
Static Factor of Safety	1.61	1.8842
Von Mises Stress	143.09 MPa	491.65 MPa
Fatigue Life	4.19×10^5 CYCLES	2.5×10^7 CYCLES
Total Deformation	0.038 mm	0.117 mm

Conclusion

The number of components (2 rockers, 1 bellcrank, 2 bolts, 2 nuts and 4 washers) was reduced into a single bellcrank without compromising on the functionality) which resulted in the new bellcrank having a mass reduction of 46.66g. By reducing the number of components, a lower tolerance build-up is achieved, better material utilization during manufacturing and lower assembly costs. Enhancement of fatigue life through the structural design of the component resulted in the new bellcrank being able to sustain 2.5×10^7 cycles as compared to the old one which could endure 4.19×10^5 cycles. Enhancement of fatigue life of the bellcrank can greatly reduce failure due to fatigue which reduces the chances of the suspension system failing.

References

1. Sarah Jalal Mosa, Effect of different quenching media on mechanical properties of AISI 1018 low carbon steel, Journal of Mechanical Engineering Research and Developments, May 2019, ISSN: 1024-1752
2. Hovorun T. P, Berladir K. V, Pererva V. I, Rudenko S. G, Martynov A. I, Modern Materials for Automotive Industry, Journal of Engineering Sciences, Volume 4, Issue 2, 2017, DOI: 10.21272
3. K. Mohan, J.A. Suresh, Palaniappan Ramu, and R. Jayaganthan, Microstructure and Mechanical Behavior of Al 7075-T6 Subjected to Shallow Cryogenic Treatment, ASM International, February 2016, DOI: 10.1007
4. F. Hussain, S. Abdullah and M.Z. Nuawi, Effect of temperature on fatigue life behavior of aluminium alloy AA6061 using analytical approach, Journal of Mechanical Engineering and Sciences, Volume 10, Issue 3, December 2016, ISSN: 2231-8380
5. M. Janecek, F.Novy, P.Harcuba, J. Strasky, L Trsko, M. Mhaede and L Wagner, The Very High Cycle Fatigue Behaviour of Ti-6Al-4V Alloy, International Symposium on Physics of Materials , Volume 128, 2015, DOI: 10.12693
6. K. Shinozawa, H. Kobayashi, M. Terada and A.Matsui, Effect of anodized coatings on fatigue strength in Aluminium alloy, Engineering Sciences Volume 33, 2001, ISSN 17433533
7. Ren Rui, Bian Gong and Zhigang Fang, Force and strength analysis of FSAE racing suspension based on spatial analytic geometry, IOP Conf. Series: Materials Science and Engineering, 2019, DOI: 10.1088
8. Maciej Szulca, Ireneusz Malujdaa and Krzysztof Talaśkaa, Method of determination of safety factor on example of selected structure, 20th International Conference: Machine Modeling and Simulations, 2016, DOI: 10.1016
9. Richard G. Budynas and J. Keith Nisbett, Shigley's Mechanical Engineering Design, 9th Edition, published by McGraw-Hill, Page 2-265, ISBN-13: 978-8121905015
10. R.S Khurmi and J.K Gupta, A Textbook of Machine Design (S.I. Units), Eurasia Publishing House PVT. LTD., 2005, Page 558-600, ISBN: 978–0–07–352928–8
11. K. Mahadevan and K. Balaveera Reddy, Design Data Handbook for Mechanical Engineers in S.I. and Metric Units, 4th Edition, CBS Publishers& Distributors Pvt Ltd., 2013, ISBN: 978-81-239-2315-4
12. Jakub Mesicek, Marek Pagac, Jana Petru, Petr Novak, Jiri Hajnys, Kristyna Kutiova. Topological Optimization of The Formula Student Bell Crank. DOI: 10.17973/MMSJ.2019_10_201893 (MM Science Journal, Oct 2019). (pp:29642966)
13. Zhu J, Gao T. Topology Optimization in Engineering Structure Design. London: ISTE Press - Elsevier; ISBN: 978-1-78548-224-3; December 2016
14. Aykut Kentli.Topology Optimization Applications on Engineering Structures. DOI: 10.5772/intechopen.90474, Peer reviewed 2019, Published: Dec 2019.
15. ANSYS Theory Reference, Release 5.6. Product manual. Eleventh Edition.
16. Ikpe Aniekan, Owunna Ikechukwu and P.O. Ebunilo, Redesign of a Bell Crank to Ensure Compliance with Von-mises Failure Criterion, International Journal of Scientific & Engineering Research, Volume 7, Issue 5, May-2016, ISSN 2229-5518
17. Byeong-Sam Kim, Kyoungwoo Park, Kinematic Motion Analysis and Structural Analysis of Bellcrank Structures Using FEM, Journal of Software Engineering and Applications, 2013, Vol.6, pp.49-55
18. Ajay Kumar, Rahul Rajput, Amit Nagar, Hirdesh Gautam and Gaurav Saxena, Design and Analysis of Suspension Components of F1 Prototype, International Journal for Scientific Research & Development| Vol. 5, Issue 03, 2017, ISSN: 2321-0613, pp.495496
19. Ashish Avinash Vadhe, Design and Optimization of Formula SAE Suspension system, International Journal of Current Engineering and Technology, May 2018, Vol.8, Isuue.3, 2018, ISSN: 2277 – 4106, pp. 617-618
20. Mohammed Rahall Masood, Mohammed Moizuddin, Akbar Hussain, Design optimization of bell crank lever, International